ChemComm

Accepted Manuscript

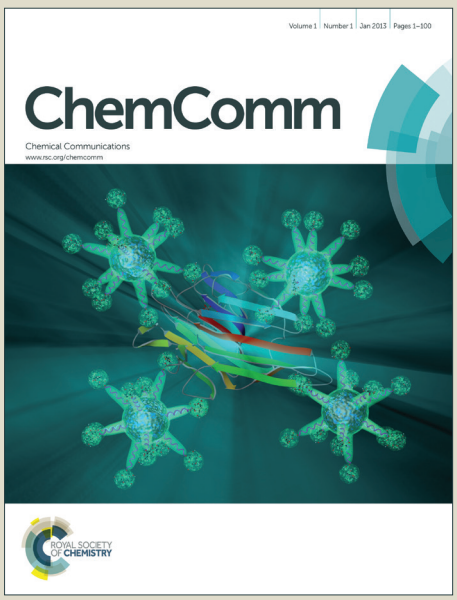

ROYAL SOCIETY OF CHEMISTRY

www.rsc.org/chemcomm

Journal Name

COMMUNICATION

Intumescent flame retardant-derived P,N co-doped porous carbon as an efficient electrocatalyst for the oxygen reduction reaction

Received 00th January 20xx,
Accepted 00th January 20xx

DOI: 10.1039/x0xx00000x

www.rsc.org/

Yinling Wang,*[a] Xuemei Zhang,[a] Anna Li[a] and Maoguo Li*[a]

Intumescent flame retardants (IFRs) including melamine (MA), ammonium polyphosphate (APP), and polydopamine (PDA), were utilized as the precursor to prepare P,N co-doped hierarchically porous carbon which exhibits high electrocatalytic activity and durability for the oxygen reduction reaction (ORR). This finding indicates that ingenious design of the precursor can lead to functional carbon materials with a simple process.

It has been a great challenge to develop efficient, stable and low-cost electrocatalysts for the oxygen reduction reaction (ORR), which is an important cathodic reaction for the energy conversion devices such as fuel cells[1] and metal-air batteries.[2] Recently heteroatom (e.g., N,B,S) doped carbon materials are attractive for their excellent catalytic activity among the substituted catalysts for the effective but expensive Pt-based catalysts.[3] The possible reason for the high catalytic activity may be that heteroatom can activate the π electrons of sp^2 carbon materials and create charged-sites favorable for O_2 adsorption.[4] The adsorbed O_2 molecules have weaker bond energy, which is beneficial to reduce the activation energy of the ORR.[5] Moreover, some studies reveal that the ORR catalytic activity can be further enhanced by co-doping carbon with S-N,[6] B-N,[7] and P-N[8] etc.

Generally, co-doped carbon combined with porous structure may be the more promising catalysts because the porous structure can not only offer larger surface areas to expose abundant active sites but also accelerate the mass transfer. At present, the doping can be achieved by processing prepared graphitic carbon materials using heteroatom-contained dopants[9] or directly pyrolyzing heteroatom-contained precursors.[10] Obviously, the latter doping method is easier to be operated for the simultaneous formation of carbon and doping with heteroatom. Heteroatom doped porous carbon materials are mainly prepared by template method[11] or post-activation method,[12] which are complex for the necessary template removal process or post treatment. Therefore, one-step procedure for the formation, doping and hole-forming of carbon is expected for scale production of catalysts, which can be achieved by the reasonable design of the precursors.

On the other hand, intumescent flame retardants (IFRs) are highly efficient and environmentally friendly fire retardants which are widely used in flame retardant coating. IFRs will be expanded when they are exposed to a sufficiently high temperature and form a porous char to establish a protective coating for the base material.[13] IFRs are composed of three parts: (1) a carbon source (e.g., pentaerythritol) to form carbon, (2) an acid source (e.g., ammonium polyphosphate) to catalyze the dehydration and carbon-forming of carbon sources and (c) a gas source (e.g., melamine) to supply gas and form pores. Although IFRs are intensively studied in the field of fire chemistry, they are less known in the field of material chemistry. Therefore, it is an exciting work to imitate such a system to prepare heteroatom doped porous carbon.

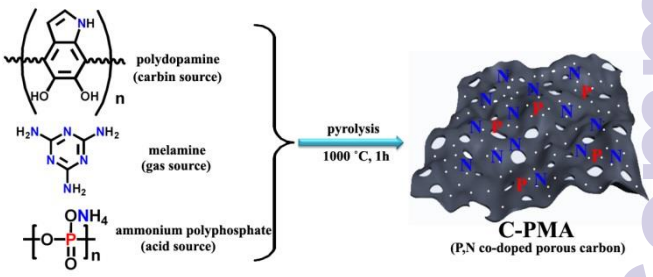

Scheme 1 Illustration of the preparation of C-PMA.

Herein we report a facile one-step pyrolysis method to prepare P,N co-doped carbon material with porous structure using melamine (MA), ammonium polyphosphate (APP) and polydopamine (PDA) as precursors, which exhibits high activity as an electrocatalyst for the ORR. PDA can be obtained by the self-polymerization of nontoxic, widespread dopamine (DA),[9a] meanwhile, MA and APP are both commercial

[a] The Key Laboratory of Functional Molecular Solids, Ministry of Education, Anhui Key Laboratory of Chemo-Biosensing, College of Chemistry and Materials Science, Anhui Normal University, Wuhu 241000, People's Republic of China. E-mail: wyinl@mail.ustc.edu.cn (Y. Wang); limaoguo@mail.ahnu.edu.cn (M. Li)

† Electronic Supplementary Information (ESI) available: Experimental, additional SEM images, BET and electrocatalytic data are included. See DOI: 10.1039/x0xx00000x

available and low-cost, which makes this method more practical. Similar to the IFRs, in our system, PDA is the carbon source and nitrogen source, APP is the P and N source and the catalyst for the dehydration, and MA is the pore-forming agent and N source. The process for the preparation of P,N co-doped porous carbon material (denoted as C-PMA) is shown in Scheme 1.

Typically, the mixture of PDA, MA and APP was first obtained by the self-polymerization of 1 g DA in the presence of 25 g MA and 150 mg APP at a pH 8.5 Tris-buffer solution (for experimental details, see ESI†). Then the dried mixture was subjected to a pyrolysis at 1000 ˚C for 1h.

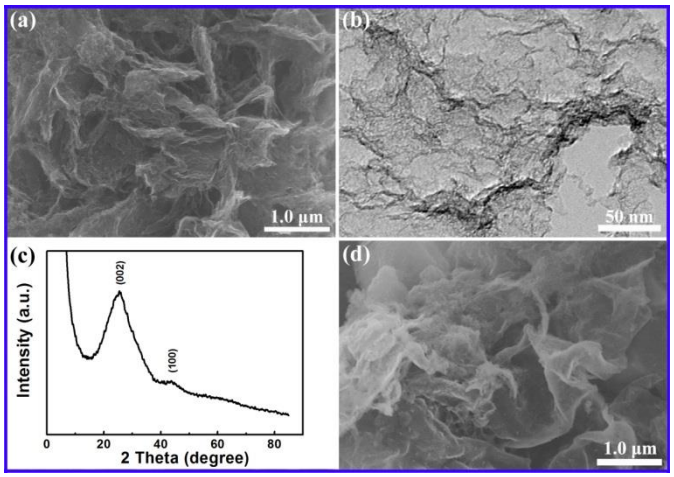

Fig. 1 (a) SEM, (b) TEM images and (c) XRD pattern of C-PMA pyrolyzed at 1000 ˚C. (d) SEM images of C-PMA pyrolyzed at 700 ˚C.

The morphology of the resulting materials was characterized by SEM and TEM. The SEM image (Fig. 1a) reveals the porous structure of C-PMA with the pore size of several hundreds of nanometers. Compared with the SEM images of the carbon materials derived from PDA (denoted as C-P), PDA/APP (denoted as C-PA) and PDA/MA (denoted as C-PM), it can be concluded that MA plays a great role in the formation of the porous structure. The TEM image (Fig. 1b) further proves the macroporous structure and the formation of crumpled graphene-like sheets. Fig. 1c shows the XRD pattern of C-PMA. The peaks appearing at 25 ° and 44 ° correspond to (002) and (100) reflections of graphitic carbon, respectively.[6]

It has been reported that the degradation of APP at above 200 ˚C results in a highly condensed polyphosphoric acid and the azeotropic P_4O_{10}-H_2O mixture boils above 600 ˚C.[14] Therefore, we infer that the interface between the liquid of P_4O_{10}-H_2O and the melt PDA lead to the graphene-like sheets. Considering that 1000 ˚C is too high and the liquid of P_4O_{10}-H_2O disappears in a short time, the morphology of the samples treated at 700 ˚C was also investigated. As expected, the graphene-like sheets are more remarkable at 700 ˚C (Fig. 1d), confirming the key role of APP for the formation of graphene-like sheets.

The electronic structure of the carbon materials was explored by Raman spectra (Fig. 2 a). The peaks at 1580 cm^{-1} (G-band) and 1350 cm^{-1} (D band) confirm the co-existence of graphitic carbon and disordered carbon.[15] The graphitic carbon can offer high electrical conductivity and the disordered carbon can provide active sites,[16] which are both beneficial to the electrocatalysis of the ORR. To get the composition information, the C-PMA was further characterized by XPS. The elemental composition of C-PMA combined with that of C-P, C-PM is listed in Table 1. It can be seen that the elements N and P were successfully doped into C-PMA. Moreover, the content of N increases in the order of C-P, C-PM and C-PMA, implying that PDA, MA and APP are all N source for the doped carbon materials. However, the content of P is very low, which may be due to the volatilization of phosphorus at high temperature. In addition, the content of element O for C-PMA is the lowest, which may be attributed to the dehydration of APP.

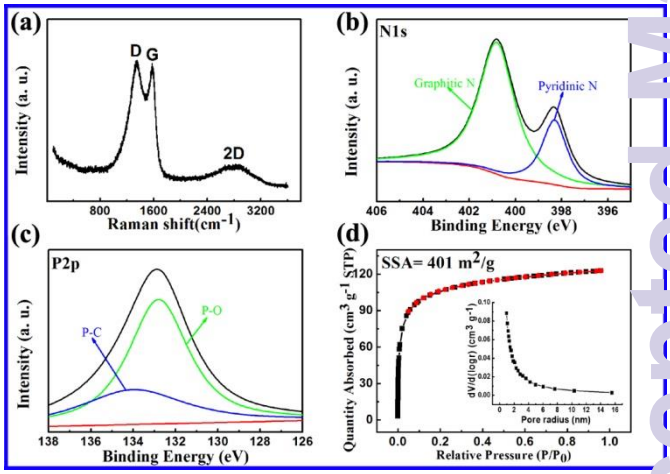

Fig. 2 (a) Raman spectrum, (b) High resolution XPS spectra of N1s, (c) High resolution XPS spectra of P2p, and (d) N_2 adsorption-desorption isotherm and the corresponding BJH pore size distribution curve (inset) of C-PMA pyrolyzed at 1000 ˚C.

Table 1 Elemental composition of the resulted carbon material from XPS analysis.

Sample	C (atom %)	N (atom %)	O (atom %)	P (atom %)
C-P	93.59	2.79	3.62	-
C-PM	91.61	5.26	3.13	-
C-PMA	90.64	6.54	2.56	0.26

The N1s spectrum (Fig. 2b) indicates that the element N exists in the form of graphitic-N (400.8 eV) and pyridinic-N (398.3 eV) which both have great contributions to the catalytic activity. In contrast, the form of pyrrolic-N (399.5 eV), showing low catalytical activity toward ORR,[6,9a] is not found, quite similar to those reported elsewhere.[17] The pyrrolic N can transform to graphitic N at high temperatures.[17b] The fitted P2p spectrum (Fig. 2c) shows two peaks at 132.8 and 134.0 eV, indicating the presence of P-O and P-C, respectively.[18] The co-doping of P and N in C-PMA may endow this carbon material with high ORR activity for the synergistic effect.[19]

Nitrogen adsorption-desorption measurements were conducted to access the porous structure and the specific surface area of C-PMA. As shown in Fig. 2d, the N_2 adsorption-desorption isotherm exhibits a typical type I profile with no hysteresis loop, characteristic of a microporous

Journal Name

COMMUNICATION

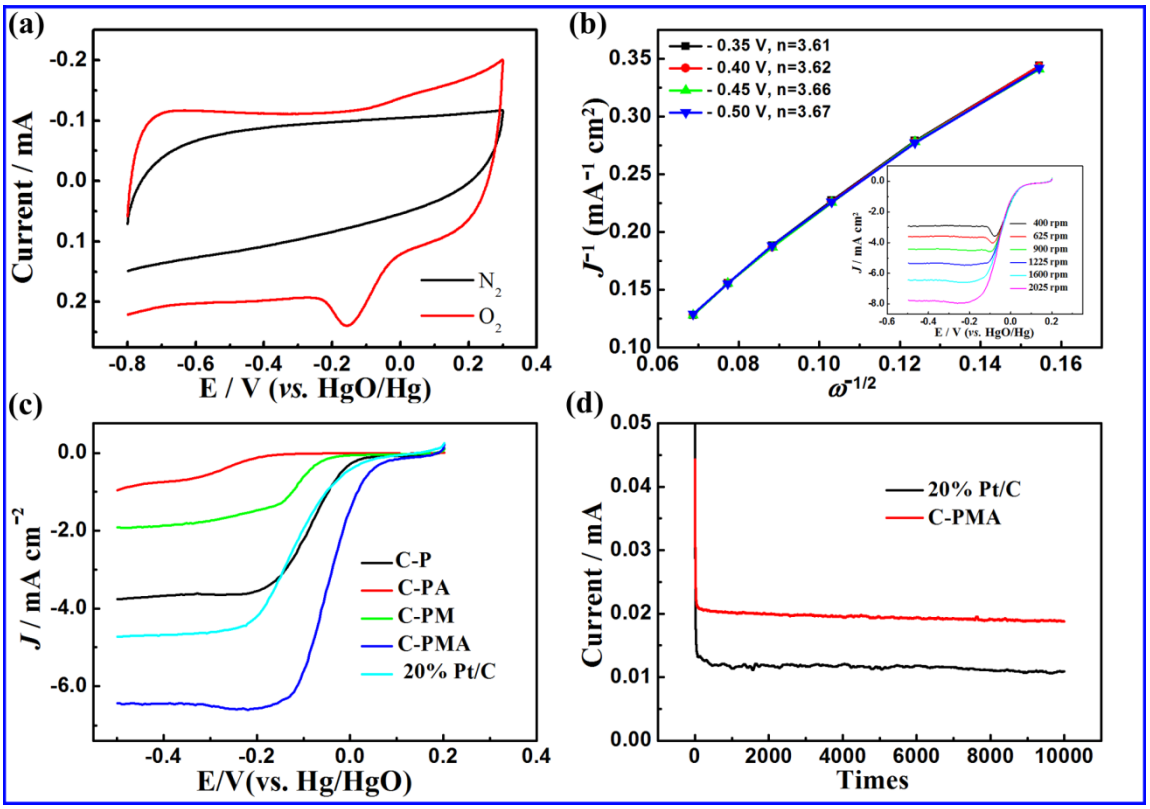

Fig. 3 Electrocatalytic activity for the ORR of C-PAM obtained at 1000 ˚C. (a) CV curves in a N_2- and O_2-saturated 0.1 M KOH solution at a scan rate of 50 mV s^{-1}, (b) Koutecky−Levich plots (J^{-1} versus $\omega^{-1/2}$) at different electrode potentials (inset: LSV curves at different rotation rates), (c) LSV curves of different electrocatalysts at a disk rotating rate of 1600 rpm and a scanning rate of 10 mV s^{-1}, and (d) Durability evaluation of C-PMA in O_2-saturated 0.1 M KOH solution at −0.3V.

material. From the corresponding pore size distribution cure inserted in Fig. 2d, it can be seen that the radius of the pore are mainly in the rage of 0-2 nm. The C-PMA displays a large Brunauer-Emmett-Teller (BET) specific surface area (SSA) of 401 m^2 g^{-1}. The micropore surface area calculated from *t*-plots is 231 m^2 g^{-1} and the external surface area of 171 m^2 g^{-1} may be attributed to the macropore induced by MA. In addition, the N_2 adsorption-desorption isotherm of C-P and C-PM is shown in Fig. S2 (EIS †) and the corresponding SSA can be seen at Table S1 (EIS †). It should be noted that the BET specific surface area of C-PMA is larger than that of C-PM (296 m^2 g^{-1}) but smaller than that of C-P (483 m^2 g^{-1}). We suppose that the reason that the SSA of C-PMA is higher than that of C-PM may own to the activation of P_4O_{10}-H_2O mixture derived from APP during the pyrolysis process. At the same time, from the BET results and the SEM image of C-P, it can be inferred that the pores assembled by carbon spheres result in the high SSA of C-P. In a word, the hierarchically porous structure and the large SSA of C-PMA are advantageous to the ORR catalytic activity.

The electrocatalytic activity of C-PMA was first investigated by cyclic voltammetry (CV) in N_2- and O_2-saturated 0.1 M KOH solution at a scan rate of 50 mV s^{-1}. As shown in Fig. 3a，an extra single cathodic reduction peak at −0.15 V (vs. HgO/Hg) appears in O_2-saturated 0.1 M KOH solution compared with that in N_2-saturated 0.1 M KOH solution, indicating the obvious the ORR catalytic activity of C-PMA. It should be noted that the ORR catalytic activity of C-PMA was strongly depend on the pyrolysis temperature and mass ratio of DA, MA and APP. Fig. S3 (EIS †) shows the results of optimal experiments. The C-PMA with best ORR catalytic activity was obtained when the pre-treated mixture of 1 g DA, 25 g MA and 0.15 g APP was pyrolyzed at 1000 ˚C for 1 h.

The mechanism of ORR on the C-PMA modified electrode was further studied by the linear-sweep voltammetry (LSV) at a rotating disk electrode in O_2-saturated 0.1 M KOH solution. The inset in Fig. 3b shows the LSV curves at different rotating rates, from which the corresponding Koutecky-Levich p

were calculated at investigated potential (Fig. 3b). From the slops of koutecky-Levich plots with good linearity, the transferred electron number (n) was obtained via the K-L equation.[20] The average transferred electron number is larger than 3.6 at the investigated potential, which is close to that of commercial 20% Pt/C (n = ~3.9, the corresponding LSV curves and Koutecky-Levich plots of Pt/C are shown in Fig. S4. EIS †). This result indicates that the ORR is 4*e* dominant pathway. The direct 4*e* pathway for the ORR is the desirable pathway for its high utilization efficiency of electrons and the absence of intermediate hydroperoxide to degrade the catalysts or the corresponding components.

Fig. 3c displays the LSV curves of different electrocatalysts at 1600 rpm. Comparing whatever in the aspect of onset potential or of limiting current, the C-PMA exhibits superior ORR performance to C-P, C-PM, C-PA (carbon material derived from PDA and APP) and even commercial 20% Pt/C. As a catalyst for the ORR, the onset potential significantly reflects the O_2 reduction overpotential. The C-PMA electrode shows an onset potential of ~0.112 V, more positive than that of 20% Pt/C (~0.079 V). At the same time, the half-wave potential of the C-PMA modified electrode is also more positive than that of the 20% Pt/C catalyst. The ORR onset potential demonstrated with the C-PMA catalyst is superior to most reported values for C-based ORR catalysts, which seldom have the more positive onset potential than that of Pt/C.[16,21] The excellent ORR catalytic activity of C-PMA can be related to its hierarchically porous structure, high specific surface area, the co-doping of N,P and the formation of graphic carbon.

The durability of C-PMA modified electrode was also evaluated by chronoamperometry. Fig. 3d shows the *i-t* curve in an O_2-saturated 0.1 M KOH solution at −0.3 V. Compared with 20% Pt/C, the C-PMA display a better long-term stability with almost 100% retention vs. 62% retention of 20% Pt/C over 10000 s of the test. However, some small fluctuations appear in the *i-t* curve for the C-PMA and the reason remains unclear. In addition, the C-PMA modified electrode shows a better tolerance to methanol compared with 20% Pt/C (Fig. S5, EIS †), which is a necessary property for C-PMA to be used in the direct methanol fuel cells (DMFC).

In conclusion, we have prepared the P,N co-doped hierarchically porous carbon materials simply through one-step pyrolysis of the IFRs including PDA, MA and APP. The resultant carbon materials demonstrate higher ORR activity, better durability and more superior tolerance to methanol than commercial 20% Pt/C. The higher ORR activity are attributed to the hierarchically porous structure, high SSA, the co-doping of N,P and the formation of graphic carbon. The highlight of this study lies in the ensemble effects of the precursor system which accomplish the carbon-forming, pore-forming and heteroatom doping in one-step pyrolysis process. The intumescent flame retardant was first time proposed to synthesize the advanced carbon materials. We believe that the smart design of the precursor composite will be an effective solution for the simple and scale preparation of the heteroatom doped porous carbon materials.

This work is supported by Anhui Provincial Natural Scien[ce] Foundation (Grant No: 1408085QB27) and National Natur[al] Science Foundation of China (Grant No: 21075001). X.Z. an[d] A.L. are grateful for the financial support from the AH[NU] Innovation Foundation (2015cxsj141 and 2015cxsj147).

Notes and references

1 M. K. Debe, *Nature*, 2012, **486**, 43.
2 L. Dai, Y. Xue, L. Qu, H.-J. Choi and J.-B. Baek, *Chem. Rev.*, 2015, **115**, 4823.
3 (a) G. Nam, J. Park, S. T. Kim, D.-B. Shin, N. Park, Y. Kim, J.-S. Lee, J. Cho, *Nano Lett.*, 2014, **14**, 1870; (b) L. J. Yang, S. J. Jiang, Y. Zhao, L. Zhu, S. Chen, X. Z. Wang, Q. Wu, J. Ma, Y. W. Ma and Z. H., *Angew. Chem. Int. Ed.*, 2011, **50**, 7132; (c) Y. Meng, D. Voiry, A. Goswami, X. Zou, X. Huang, M. Chhowalla, Z. Liu and T. Asefa, *J. Am. Chem. Soc.*, 2014, **136**, 13554; (d) X. Sun, Y. Zhang, P. Song, Pan, L. Zhuang, W. Xu and W. Xing, *ACS Catal.*, 2013, **3**, 1726.
4 Y. Zhao, L. Yang, S. Chen, X. Wang, Y. Ma, Q. Wu, Y. Jiang, W. Qian and Z. Hu, *J. Am. Chem. Soc.*, 2013, **135**, 1201.
5 W. Ding, Z. Wei, S. Chen, X. Qi, T. Yang, J. Hu, D. Wang, L.-J. W. S. F. Alvi and L. Li, *Angew. Chem., Int. Ed.*, 2013, **52**, 11755.
6 T. X. Wu, G. Z. Wang, X. Zhang, C. Chen, Y. X. Zhang and H. J. Zhao, *Chem. Commun.*, 2015, **51**, 1334.
7 S. Y. Wang, E. Iyyamperumal, A. Roy, Y. H. Xue, D. S. Yu and L. M. Dai, *Angew. Chem., Int. Ed.*, 2011, **50**, 11756.
8 D. Yu, Y. Xue and L. Dai, *J. Phys. Chem. Letter.*, 2012, **3**, 2863.
9 (a) K. Ai, Y. Liu, C. Ruan, L. Lu and G. M. Lu, *Adv. Mater.*, 2013, **25**, 998; (b) X. M. Zhang, Y. L. Wang, S. Y. Dong and M. G. Li, *Electrochim. Acta*, 2015, **170**, 248; (c) Y. L. Wang, L. Liu, M. G. Li, S. D. Xu and F. Gao, *Biosens. Bioelectron.*, 2011, **30**, 107.
10 (a) T. Horikawa, N. Sakao, T. Sekida, J. Hayashi, D. D. Do, M. Katoh, *Carbon*, 2012, **50**, 1833; (b) M. Zhong, S. Natesakhawat, J. P. Baltrus, D. Luebke, H. Nulwala, K. Matyjaszewski, T. Kowalewski, *Chem. Commun.*, 2012, **48**, 11516; (c) S. Pandiaraj, H. B. Aiyappa, R. Banerjee and S. Kurungot, *Chem.Commun.*, 2014, **50**, 3363.
11 (a) J.-C. Yoon, J.-S. Lee, S.-I. Kim, K.-H. Kim and J.-H. Jang, *Sci. Rep.*, 2013, **3**, 1788; (b) C. Cui, W. Qian, Y. Yu, C. Kong, B. Yu, L. Xiang and F. Wei, *J. Am. Chem. Soc.*, 2014, **136**, 2256.
12 (a) Z.-S. Wu, Y. Sun, Y.-Z. Tan, S. Yang, X. Feng and K. Mullen, *J. Am.Chem. Soc.*, 2012, **134**, 19532; (b) C. Wu, X. Huang, G. Wang, L. Lv,G. Chen, G. Li and P. Jiang, *Adv. Funct. Mater.*, 2013, **23**, 506; (c) L. Chen, Y. Zhang, C. Lin, W. Yang, Y. Meng, Y. Guo, M. Li and D. Xiao, *J. Mater. Chem. A*, 2014, **2**, 9684.
13 M. C. Yewa, N. H. Ramli Sulong, M. K. Yew, M. A. Amalina and M. R. Johan, *Prog. Org. Coatings*, 2015, **81**, 116.
14 M. Jimenez, S. Duquesne and S. Bourbigot, *Thermochim. Acta*, 2006, **449**, 16.
15 S. Wang, L. Zhang, Z. Xia, A. Roy, D. W. Chang, J. B. Baek and L. Dai, *Angew. Chem. Int. Ed.*, 2012, **51**, 4209.
16 H. Jin, H. Huang, Y. He, X. Feng, S. Wang, L. Dai and J. Wang, *J. Am. Chem. Soc.*, 2015, **137**, 7588.
17 (a) Q. Liu, Y. Duan, Q. Zhao, F. Pan, B. Zhang and J. Zhang, *Langmuir*, 2014, **30**, 8238; (b) B. Zheng, J. Wang, F. Wang and X. Xia, *Electrochem. Commun.*, 2013, **28**, 24.
18 D.-S. Yang, D. Bhattacharjya, S. Inamdar, J. Park and J.-S. Yu, *J. Am. Chem. Soc.*, 2012, **134**, 16127.
19 J. Zhu , G. He , L. Liang , Q. Wan and P. K. Shen, *Electrochim. Acta*, 2015, **158**, 374.
20 R. Huo, W. Jiang, S. Xu, F. Zhang and J. Hu, *Nanoscale*, 2014, **6**, 20[illegible].
21 (a) C. You, X. Zen, X. Qiao, F. Liu, T. Shu, L. Du,J. Zeng and S. Liao, *Nanoscale*, 2015, **7**, 3780; (b) W. Yang, T. P. Fellinger and M. Antonietti, *J. Am. Chem. Soc.*, 2011, **133,** 206.